C. Swindells (iD), A. T. Hindmarch, A. J. Gallant (iD), and D. Atkinson (iD)

View Online   Export Citation   CrossMark

Spin current propagation through ultra-thin insulating layers in multilayered ferromagnetic systems

C. Swindells,[1] A. T. Hindmarch,[1] A. J. Gallant,[2] and D. Atkinson[1,a]

AFFILIATIONS

[1]Department of Physics, Durham University, Durham DH1 3LE, United Kingdom
[2]Department of Engineering, Durham University, Durham DH1 3LE, United Kingdom

[a]Electronic mail: del.atkinson@durham.ac.uk

ABSTRACT

Spin current pumping from a ferromagnet through an insulating layer into a heavy metal was studied in a $CoFeB/SiO_2/Pt$ system in relation to the thickness and interfacial structure of the insulating layer. The propagation of spin current from the ferromagnet into the heavy metal falls rapidly with sub-nanometer thicknesses of SiO_2 and is suppressed beyond a nominal thickness of 2 nm. Structural analysis shows that SiO_2 only forms a complete barrier layer beyond around 2 nm, indicating that the presence of a discontinuous insulating barrier, and not tunneling or diffusion, explains the main observations of spin-pumping with thin insulating layers.

The manipulation of spin currents across ferromagnetic (FM) and non-magnetic (NM) interfaces is key to spintronic applications and remains an active area of research.[1–3] Precessing magnetization in a ferromagnetic layer can transfer spin angular momentum, in the form of a spin current, into an adjacent NM layer,[4] a process referred to as spin pumping. One of the main manifestations of this spin pumping mechanism is an increase in the precessional damping of a system,[5–7] and while details remain to be understood, the basis of this process is well described for ferromagnetic/metallic systems.[5,8] However, the propagation of spin current through an insulating barrier has led to conflicting results in the literature. Initial theoretical predictions of spin pumping required a transparent interface between the FM and NM layers for a large increase in damping;[9] however, early experimental results by Moriyama *et al.*[10] suggested an enhancement in the damping with an insulating barrier being present. This contrasts with later works by Kim *et al.*[11] and Mosendz *et al.*,[12] who observed the suppression of spin pumping with the insertion of nano-oxide and MgO layers, respectively. Studies of both Si and oxide semiconductors[13] have also shown some suppression of spin pumping and suggest that the carriers may continue to allow spin diffusion through the barrier. Baker *et al.*[14] also observed the suppression of spin pumping but with dynamic exchange between two FM layers across the insulating barrier in CoFe/MgO/Ni trilayers. Most recently, Mihalceanu *et al.*[15] reported a rapid decrease in the damping due to reduced spin

pumping with the addition of an ultra-thin MgO barrier layer between Fe and Pt, from which it was concluded that spin current can tunnel through a few monolayers of an insulating oxide barrier. The work was supported by transmission electron microscopy (TEM) imaging, which is limited to sampling very small areas and provides a projection of a thin 3D sample volume that may not show pinhole defects, and any defects present may be difficult to directly image.[16]

The discrepancies between the previous studies may be associated with the details of the multilayered structure. In particular, the nature of the interface structure in such systems is known to be important for spin-pumping,[17,18] and in the ultra-thin film regime, the presence of a continuous intermediate layer needs to be established when studying such interlayer effects.[19] Both spin pumping and $d - d$ hybridization across a FM/NM interface lead to additional magnetic energy loss and increased precessional damping. An increase in damping linked to spin pumping across a continuous insulating layer implies some form of spin current tunneling; however, even small discontinuities, such as pinholes, within the insulating layer can allow for $d - d$ hybridization between the ferromagnetic and heavy metal (HM) layers, leading to an increase in the damping,[20,21] and limited channels for spin current propagation. A detailed understanding of the role of the structure at the interface is therefore needed to fully characterize the dynamic magnetic behavior with an insulating barrier.

This study investigates the evolution of spin-pumping from a thin-film ferromagnet into a heavy metal layer as a function of the thickness of an oxide spacer layer. The spin transport was determined by broadband ferromagnetic resonance (FMR) and the sample structure was analyzed using x-ray reflectivity (XRR) in order to understand the extent of the interfacial regions between the oxide and the FM and NM layers. The study shows here that spin pumping can be fully suppressed when a complete layer of the insulating material is formed.

The enhancement of damping by spin pumping depends upon the interface and the NM material. Spin pumping leads to spin accumulation within the NM layer that decays over a characteristic length-scale, the spin diffusion length. The transparency of the interface, which governs the efficiency of spin pumping, is characterized by the effective spin-mixing conductance.[22–24] The enhancement in damping also depends upon the thickness of both the FM and NM layers. The FM thickness dependence of the damping, α_{tot}, is commonly given by

$$\alpha_{tot} = \alpha_0 + \frac{\gamma\hbar}{4\pi M_s t_{FM}} g_{eff}^{\uparrow\downarrow}, \qquad (1)$$

with α_0 being the bulk intrinsic Gilbert damping parameter, $g_{eff}^{\uparrow\downarrow}$ the effective spin-mixing conductance, which is valid for a given NM thickness and other parameters, and γ is the gyromagnetic ratio that can be expressed in terms of the spectroscopic g-factor using $\gamma = g\mu_B/\hbar$. The largest enhancement in the damping is obtained with a combination of a small FM thickness and a large NM thickness, i.e., above the spin diffusion length. However, in multilayered systems, it may be beneficial for controlling the damping of the FM layers by manipulating the flow of spin current across interfaces. One method to achieve this may be to use insulating barriers; however, this requires the nature of spin transport associated with an insulating barrier to be understood.

Magnetron sputtering was used to grow a series of samples varying the SiO_2 thickness in a $CoFeB(10\,nm)/SiO_2(0-5\,nm)/Pt(10\,nm)$ structure, along with a reference sample with no Pt. Dynamic and direct structural measurements on the reference samples can be found in the supplementary material.

XRR was used to extract interfacial structure information. This method measures over a large area, of the order of square centimeters, unlike transmission electron microscopy, providing an averaged view of both the layers and interfaces within a sample. Figure 1 shows the examples of both the measured reflectivity data and the best-fitting simulations obtained using the GenX code.[25] The scattering length density (SLD) profiles were extracted from the best-fitting model for a sample of $CoFeB(10\,nm)/SiO_2(2\,nm)/Pt(10\,nm)$ and $CoFeB(10\,nm)/SiO_2(5\,nm)/Pt(10\,nm)$. The interface width in such multilayered structures results from a combination of the topographical roughness of the interface between the layers and some chemical intermixing between these different layers, and here, the interface width between the insulating and FM layers largely reflects chemical intermixing across the interface. A value of the interface width can be estimated from the slope of the scattering length density (SLD) where it changes from 90% to 10% of its value from one layer to the next. For the CoFeB and SiO_2 interface, this analysis gives an interface width of 2.4 nm, and below this thickness, the SiO_2 layer is discontinuous.

The damping was obtained from the measurements of magnetic field-swept FMR as a function of SiO_2 thickness. In this setup, the sample was placed face down onto an impedance-matched microstripline, driven at fixed excitation frequency, f, by an RF signal generator,
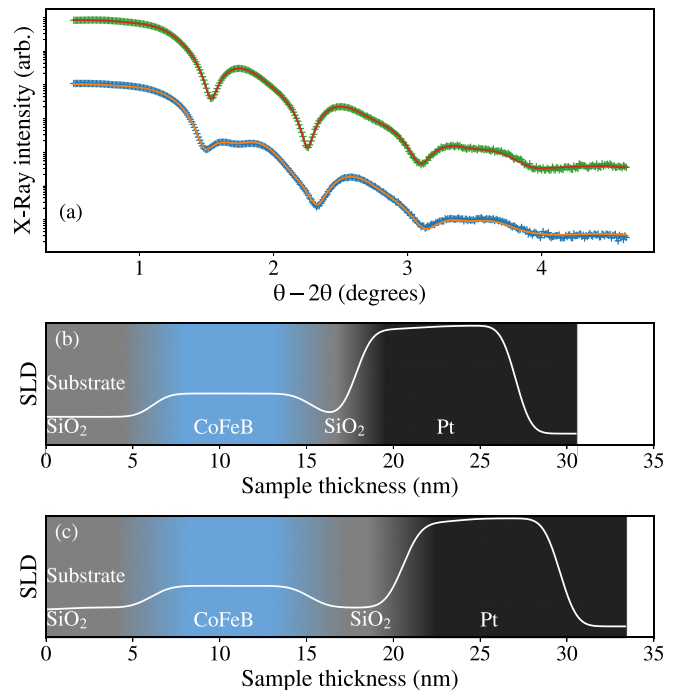

FIG. 1. (a) XRR data and best fit for $CoFeB(10\,nm)/SiO_2(2\,nm)/Pt(10\,nm)$ (top) and $CoFeB(10\,nm)/SiO_2(5\,nm)/Pt(10\,nm)$ (bottom). (b) Real part of the scattering length density (SLD) profile from the best fit to the data for the 2 nm oxide barrier. (c) Same as (b) for the 5 nm barrier.

with an external biasing magnetic field applied parallel to the transmission line and hence orthogonal to the RF excitation field. Helmholtz coils were used to modulate the bias field and the time-varying output voltage of a diode power detector across the line, proportional to the field derivative of the transmitted RF power, and hence, microwave absorption, χ'', by the sample, was measured using a lock-in amplifier. The inset in Fig. 2(a) shows typical spectra around resonance as a function of magnetic field for various excitation frequencies, f.

The relationship between the field swept linewidth, ΔH, and resonant frequency allows for the separation of intrinsic and extrinsic contributions to the damping using

$$\Delta H = \Delta H_0 + \frac{4\pi\alpha}{\gamma} f, \qquad (2)$$

where $4\pi\alpha/\gamma$ is the intrinsic linewidth and ΔH_0 is the extrinsic linewidth, which is related to defects and leads to two-magnon scattering. An example fit to the linewidth data used to separate these contributions to the damping is shown in Fig. 2(a).

The effect of increasing the thickness of a SiO_2 spacer layer on both the intrinsic and extrinsic contributions to the precessional damping in $CoFeB(10\,nm)/SiO_2(x\,nm)/Pt(10\,nm)$ multilayers is shown in Figs. 2(b) and 2(c). As the nominal thickness of the oxide layer between the ferromagnet and the heavy metal spin-sink increases, the intrinsic linewidth decreases. This decrease is at a similar rate to that observed for an MgO spacer layer.[15] The intrinsic damping decreases toward the value in the case where no spin-sink is present, as indicated in the figure by the orange square data point. No change
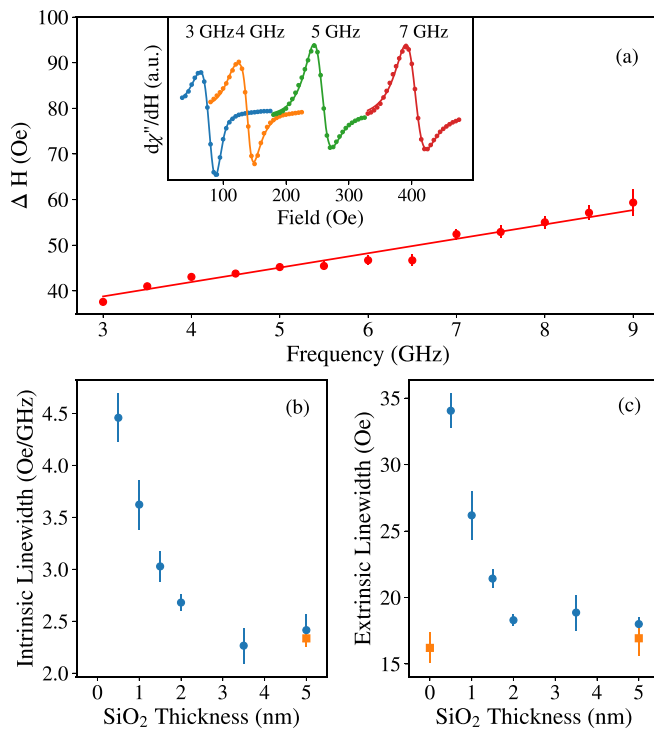
FIG. 2. (a) The inset shows absorption derivative profiles at four frequencies with fits, obtained from lock-in amplifier field-swept FMR, for CoFeB(24 nm)/Pt(10 nm)/SiO$_2$(5 nm). The rest of (a) shows the measured linewidth from field-swept FMR, fitted to Eq. (2) to extract both intrinsic and extrinsic damping contributions. (b) Decrease in intrinsic contributions to the FMR linewidth as a function of SiO$_2$ thickness for CoFeB(10 nm)/SiO$_2$(x nm)/Pt(10 nm) (blue circles) with a reference sample without platinum (orange square). (c) Decrease in extrinsic contributions as a function of SiO$_2$ thickness, where the orange square at 0 nm denotes a reference sample with no SiO$_2$, and at 5 nm, it denotes a reference sample without Pt.

FIG. 3. (a) Same as Fig. 2(b) but with extracted SLD for the 5 nm SiO$_2$ barrier from Fig. 1(c) superimposed shown in red dashed lines. The horizontal gray bar indicates the damping equivalent to that of the ferromagnetic layer only. (b) Same as Fig. 2(c) with SLD for a 5 nm SiO$_2$ barrier superimposed on top given by the red dashed line. (c) Correlation between the intrinsic and extrinsic contributions for samples without a full surface coverage of the insulating layer.

in intrinsic damping is observed by varying the SiO$_2$ thickness without a Pt layer. The continued enhancement of damping with thin insulating barrier thicknesses was previously attributed to the tunneling of spin current through the insulating spacer layer.

However, an understanding of the interfacial structure is important. As shown in Fig. 3, by superimposing the normalized structural SLD profile of the CoFeB/SiO$_2$ interface on the same nominal SiO$_2$ thickness-axis as for the damping, the relationship between the structure of the insulating layer and the measured damping response can be compared. At low SiO$_2$ thicknesses (below 2.4 nm), the SiO$_2$ layer is discontinuous, enabling some localized direct contact and $d - d$ hybridization between the ferromagnet and the heavy metal (HM), where the spacer layer is incomplete, and creates direct pathways for the propagation of spin current from the ferromagnet into the spin-sink. These two mechanisms enhance the damping above that of the pure ferromagnet[20] but decrease rapidly as the area of HM in direct contact with the FM is reduced. However, when the insulating spacer layer continuously covers the ferromagnet, above 2.4 nm, there is no measured enhancement of the intrinsic damping from the heavy metal layer.

The effects of the discontinuous interface are also observed in the SiO$_2$ thickness dependence of the extrinsic contribution to the damping, see Fig. 3(b). An increase in the extrinsic contribution to the linewidth
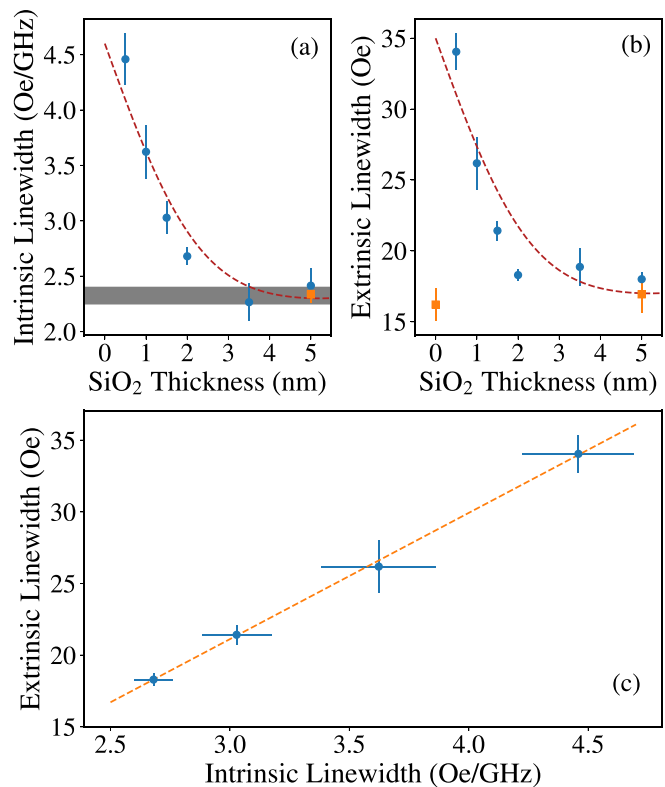
indicates an increase in defects that mediate two-magnon scattering processes. As a function of SiO$_2$ thickness, the extrinsic contribution increases in a single large step with the thinnest oxide layer and then decreases as the thickness increases further, and this decrease is comparable with the form of the scattering length density. The extrinsic contribution provides evidence further supporting the interpretation of the nominal thickness dependence as a consequence of the presence of a discontinuous insulating layer, as it has been previously shown that the discontinuous coverage of a ferromagnet with a heavy metal layer leads to enhanced extrinsic damping.[21] A slight enhancement in extrinsic damping was also found without a Pt layer, which may be attributed to the partial oxidation of the FM surface due to a discontinuous interface. The common dependence of intrinsic and extrinsic damping upon the discontinuous SiO$_2$ is further evidenced by the linear correlation between the extrinsic and intrinsic contributions for samples lacking a full surface coverage of the SiO$_2$ layer (i.e., below 2.4 nm), as shown in Fig. 3(c). Here, as discussed, regions with a low surface coverage allow for a large increase in both the extrinsic and intrinsic contributions, both of which are suppressed with the same functional form as the layer becomes complete. Direct surface measurements are unable to distinguish between defects such as pinholes, which would lead to this effect and topographical roughness, due to the lack of element specificity.

In conclusion, the link between the structure of the interface and the spin transport with a SiO_2 spacer layer was examined. It was found that spin-pumping was observed for nominal SiO_2 thicknesses up to around 2 nm, but this correlates with the length-scale corresponding to the interface width of the barrier, such that structurally the insulating layer was discontinuous when spin-pumping was observed and no enhancement of the damping was measured when the SiO_2 layer was complete (>2.4 nm). Thus, the experimentally observed spin-pumping signals with ultra-thin insulators are due to the discontinuous insulating layer rather than requiring models involving tunneling of pure spin-current. The incomplete SiO_2 layer also leads to enhanced extrinsic damping resulting from direct coupling between the FM and HM layers when the insulating layer is discontinuous. It is also shown that when the SiO_2 layer is continuous, it represents a significant barrier to spin transport, which allows for the suppression of spin current in multilayered structures.

See the supplementary material for dynamic and direct structural measurements on $CoFeB/SiO_2$ bilayers.

REFERENCES

[1] I. Zutic, J. Fabian, and S. D. Sarma, Rev. Mod. Phys. **76**, 323 (2004).

[2] A. Hoffmann, IEEE Trans. Magn. **49**, 5172 (2013).

[3] S. Azzawi, A. T. Hindmarch, and D. Atkinson, J. Phys. D **50**, 473001 (2017).

[4] J. Li, L. R. Shelford, P. Shafer, A. Tan, J. X. Deng, P. S. Keatley, C. Hwang, E. Arenholz, G. van der Laan, R. J. Hicken, and Z. Q. Qiu, Phys. Rev. Lett. **117**, 076602 (2016).

[5] Y. Tserkovnyak, A. Brataas, and G. E. Bauer, Phys. Rev. B **66**, 224403 (2002).

[6] J. C. Rojas-Sánchez, N. Reyren, P. Laczkowski, W. Savero, J. P. Attané, C. Deranlot, M. Jamet, J. M. George, L. Vila, and H. Jaffrès, Phys. Rev. Lett. **112**, 106602 (2014).

[7] M. Caminale, A. Ghosh, S. Auffret, U. Ebels, K. Ollefs, F. Wilhelm, A. Rogalev, and W. E. Bailey, Phys. Rev. B **94**, 014414 (2016).

[8] C. Swindells, A. T. Hindmarch, A. J. Gallant, and D. Atkinson, Phys. Rev. B **99**, 064406 (2019).

[9] A. Brataas, Y. Tserkovnyak, G. E. W. Bauer, and B. I. Halperin, Phys. Rev. B **66**, 060404 (2002).

[10] T. Moriyama, R. Cao, X. Fan, G. Xuan, B. K. Nikolić, Y. Tserkovnyak, J. Kolodzey, and J. Q. Xiao, Phys. Rev. Lett. **100**, 067602 (2008).

[11] D. H. Kim, H. H. Kim, and C. Y. You, Appl. Phys. Lett. **99**, 072502 (2011).

[12] O. Mosendz, J. E. Pearson, F. Y. Fradin, S. D. Bader, and A. Hoffmann, Appl. Phys. Lett. **96**, 022502 (2010).

[13] C. H. Du, H. L. Wang, Y. Pu, T. L. Meyer, P. M. Woodward, F. Y. Yang, and P. C. Hammel, Phys. Rev. Lett. **111**, 247202 (2013).

[14] A. A. Baker, A. I. Figueroa, D. Pingstone, V. K. Lazarov, G. Van Der Laan, and T. Hesjedal, Sci. Rep. **6**, 35582 (2016).

[15] L. Mihalceanu, S. Keller, J. Greser, D. Karfaridis, K. Simeonidis, G. Vourlias, T. Kehagias, A. Conca, B. Hillebrands, and E. T. Papaioannou, Appl. Phys. Lett. **110**, 252406 (2017).

[16] A. Thomas, V. Drewello, M. Schäfers, A. Weddemann, G. Reiss, G. Eilers, M. Münzenberg, K. Thiel, and M. Seibt, Appl. Phys. Lett. **93**, 152508 (2008).

[17] M. Tokaç, S. A. Bunyaev, G. N. Kakazei, D. S. Schmool, D. Atkinson, and A. T. Hindmarch, Phys. Rev. Lett. **115**, 056601 (2015).

[18] A. Ganguly, S. Azzawi, S. Saha, J. A. King, R. M. Rowan-Robinson, A. T. Hindmarch, J. Sinha, D. Atkinson, and A. Barman, Sci. Rep. **5**, 17596 (2015).

[19] R. M. Rowan-Robinson, A. A. Stashkevich, Y. Roussigné, M. Belmeguenai, S. M. Chérif, A. Thiaville, T. P. Hase, A. T. Hindmarch, and D. Atkinson, Sci. Rep. **7**, 16835 (2017).

[20] E. Barati, M. Cinal, D. M. Edwards, and A. Umerski, Phys. Rev. B **90**, 014420 (2014).

[21] S. Azzawi, A. Ganguly, M. Tokaç, R. M. Rowan-Robinson, J. Sinha, A. T. Hindmarch, A. Barman, and D. Atkinson, Phys. Rev. B **93**, 054402 (2016).

[22] W. Zhang, W. Han, X. Jiang, S. H. Yang, and S. S. Parkin, Nat. Phys. **11**, 496 (2015).

[23] O. R. Sulymenko, O. V. Prokopenko, V. S. Tiberkevich, A. N. Slavin, B. A. Ivanov, and R. S. Khymyn, Phys. Rev. Appl. **8**, 064007 (2017).

[24] M. Weiler, M. Althammer, M. Schreier, J. Lotze, M. Pernpeintner, S. Meyer, H. Huebl, R. Gross, A. Kamra, J. Xiao, Y. T. Chen, H. Jiao, G. E. Bauer, and S. T. Goennenwein, Phys. Rev. Lett. **111**, 176601 (2013).

[25] M. Björck and G. Andersson, J. Appl. Crystallogr. **40**, 1174 (2007).